

Article

Effect of Elevated Temperature on the Behavior of Amorphous Metallic Fibre-Reinforced Cement and Geopolymer Composites

Faiz Uddin Ahmed Shaikh ^{1,*}, Narwinder Singh Kahlon ¹ and Attiq Ur Rahman Dogar ²¹ School of Civil and Mechanical Engineering, Curtin University, Perth, WA 6102, Australia² Department of Civil Engineering, University of Central Punjab, Lahore 54000, Pakistan

* Correspondence: s.ahmed@curtin.edu.au

Abstract: To improve the tensile, flexural, and ductility properties of geopolymer composites, amorphous metallic fibres (AMF) are used to reinforce these composites, and the behavior of these composites at elevated temperatures has been assessed in this study. Four types of composites, i.e., cement, reinforced cement, geopolymer, and reinforced geopolymer composites have been prepared. The composites have been reinforced using AMF with a fibre volume fraction of 0.75%. The composites have been assessed for change in mass loss, cracking, compressive strength, and flexural strength at four elevated temperatures of 200 °C, 400 °C, 600 °C, and 800 °C, and conclusions have been drawn concerning these composites. The results have shown that an increase in temperature has an adverse effect on these composites, and geopolymer composites exhibit higher performance than their counterpart cement composites at elevated temperatures. The mass loss and surface cracking were significantly lower in geopolymer composites, and the fibre reinforcement had a negligible effect on mass loss. Also, the residual compressive and flexural strength of reinforced geopolymer composites was significantly higher than that of the reinforced cement composites. In addition, scanning electron microscopic images also showed that even at higher temperatures, the geopolymer matrix is present on the AMF fibre, which results in higher residual strength than the cement composites in which a negligible amount of matrix is present on the fibres.



Citation: Shaikh, F.U.A.; Kahlon, N.S.; Dogar, A.U.R. Effect of Elevated Temperature on the Behavior of Amorphous Metallic Fibre-Reinforced Cement and Geopolymer Composites. *Fibers* **2023**, *11*, 31. <https://doi.org/10.3390/fib11040031>

Academic Editors: Ionela Andreea Neacsu, Alexandru Mihai Grumezescu and Akanshu Sharma

Received: 22 November 2022

Revised: 22 February 2023

Accepted: 23 March 2023

Published: 28 March 2023



Copyright: © 2023 by the authors. Licensee MDPI, Basel, Switzerland. This article is an open access article distributed under the terms and conditions of the Creative Commons Attribution (CC BY) license (<https://creativecommons.org/licenses/by/4.0/>).

Keywords: amorphous metallic fibres (AMF); geopolymer concrete; elevated temperature; residual strength; compressive strength; flexural strength; scanning electron microscope (SEM)

1. Introduction

Concrete, being the most widely used construction material, utilizes ordinary Portland cement (OPC) as a binder and the production of cement alone is responsible for around 5 to 7% of CO₂ emissions worldwide [1]. The huge carbon footprint and large amount of energy required to produce cement have resulted in serious concerns about its environmental and economic sustainability, and researchers have started to look for environmentally friendly and sustainable supplementary cementitious materials (CSM). This quest has led to the use of cementless geopolymer binders [2], the inorganic polymers which are rich in silica and alumina and develop binding characteristics when combined with alkali activators [3]. Out of a wide variety of materials that can replace cement as a binder material, fly ash geopolymer is gaining popularity because of its worldwide availability and excellent binding properties [4]. Also, its production requires 60% less energy and emits 80% less CO₂ compared to OPC [5,6]. In addition to being sustainable and environmentally friendly, it improves the workability, strength, and durability of concrete along with reducing its drying shrinkage [7–10]. A significant amount of research studies have already been performed to assess the behavior of fly ash-based geopolymer concretes [11–17].

Even though the geopolymer concretes made with fly ash exhibit superior mechanical and durability characteristics, there are issues related to the lower tensile strength and inherent brittleness that impede the large-scale application of geopolymer composites. To

improve these properties, randomly oriented short fibres of various types, including steel, carbon, glass, PVA, PE, natural fibres, etc. are used. Out of these fibres, steel fibres are widely adopted for reinforcing geopolymer composites, and they significantly improve the mechanical properties of geopolymer concrete. However, the steel fibres are susceptible to corrosion, especially in the structures built in coastal areas and the structures exposed to repeated wetting and drying cycles. To address this issue, without compromising the strength, amorphous metallic fibres (AMF) have been recently introduced to reinforce cement and geopolymer composites and have already proved to have superior mechanical properties [18–22]. In addition to improving strength and durability, these fibres are sustainable and environmentally friendly, as their production results in 20% less CO₂ emissions than steel fibres. To further improve the mechanical properties of geopolymer composites, heat curing is used in which the composite is cured at the temperature ranges of 60 °C–80 °C for an initial 24 h. The increased properties in heat curing are achieved due to a faster geopolymer reaction [23] and lower porosity [24,25].

Although the strength and durability of AMF reinforced geopolymer concrete are well established, the behavior of AMF reinforced geopolymer concrete at elevated temperatures is still unexplored. Normally geopolymers composites possess relatively higher fire resistance than OPC owing to their chemical composition and are preferred as thermal insulators and heat resistant materials [26–30]. The structural stability and strength of hydration products in OPC concrete, i.e., calcium silicate hydrate (C-S-H) and calcium hydroxide (CH), are reduced at higher temperatures. On the other hand, in geopolymer composites, sodium aluminosilicate gels (N-A-S-H) are produced due to the reaction between aluminosilicate materials and alkali activators, which sustains the composite's strength and stability at higher temperatures [31]. Extensive studies have already been performed on geopolymer composites made with a range of source materials and alkali activators [32–37]. The performance of these composites at elevated temperatures can be further improved by reinforcing them with various organic and inorganic fibres. Through the comparison of basalt and poly-vinyl alcohol (PVA) fibres, Masi et al. [38] concluded that basalt fibres are better at sustaining the mechanical properties at elevated temperatures. The use of basalt fibres reinforced geopolymer concrete at elevated temperatures has also been recommended by Fiore et al. [39] and Welter et al. [40]. Another alternative is carbon fibres; their use at elevated temperatures has been tested and recommended by Hosan et al. [41] and Zhang et al. [42]. Hosan et al. [41] also compared the efficacy of potassium and sodium based alkali activators and concluded that potassium-based activators are better in terms of residual compressive strength, volumetric shrinkage, and mass loss.

Since amorphous metallic fibres (AMF) have emerged as an efficient alternative to the steel fibres to enhance the durability and sustainability of geopolymer composites, it is imperative to study the behavior of AMF reinforced geopolymer composites at elevated temperatures. To date, no study has been performed on this composite at elevated temperatures; therefore, an effort has been made in this study to fill this research gap. In this study, the behavior of unreinforced and AMF reinforced cement and geopolymers composites at ambient and elevated temperatures of 200 °C, 400 °C, 600 °C, and 800 °C has been studied in terms of mass loss, cracking behavior, compressive strength, flexural strength, and flexural toughness, and comparisons have been drawn between both types of composites. In addition, scanning electron microscopic (SEM) analysis has been conducted to assess the microstructure behavior of these types of composites to explain their behavior at elevated temperatures.

2. Experimental Program

2.1. Materials

The cement composite samples were prepared using ordinary Portland cement (OPC) as a binder while Class F fly ash was used as a binder for geopolymer composite. The chemical compositions of both the OPC and fly ash are given in Table 1. For the fine aggregates, natural silica sand was used in saturated and surface dried conditions before

preparing the mixes. Fineness modulus of fine aggregate (natural sand) was 1.8 and the maximum aggregate size of sand was 1.18 mm. The amorphous metallic fibres (AMF), as well as the alkali activators used in this research study, are similar to the ones used by the authors' other study [35]. The length, width, and thickness of the AMF were 15 mm, 1 mm, and 24 μm , respectively. The tensile strength and elastic modulus of the AMF were 1800 MPa and 140 GPa, respectively [18]. A photo of AMF is shown in Figure 1. The alkali activator consisted of an 8-M sodium hydroxide (NaOH) solution blended with D-grade sodium silicate (Na_2SiO_3) solution. The ratio of sodium silicate to sodium hydroxide was constant at 2.5 in all composites. The ratio of sodium silicate to sodium hydroxide solution and the molarity of sodium hydroxide used in this study are based on the authors' previous study [18], as these are the optimum alkali content for geopolymer concrete.

Table 1. Chemical composition and physical properties of OPC and Class F fly ash in *wt.%* [18].

Chemical Composition	OPC	Class F Fly Ash
SiO_2	21.10	51.11
Al_2O_3	5.24	25.56
Fe_2O_3	3.10	12.48
CaO	64.39	4.3
MgO	1.10	1.45
K_2O	0.57	0.7
Na_2O	0.23	0.77
SO_3	2.52	0.24
LOI	1.22	0.57
Particle size	25–40% $\leq 7 \mu\text{m}$	50% of 10 μm
Specific gravity	2.7	2.35–2.4



Figure 1. Amorphous Metallic Fibres used in this study ([18]). [Reproduced with permission from publisher].

2.2. Specimen Preparation

2.2.1. Casting and Curing

For preparing the composites, a Hobart mixer with a 10-L capacity was used. The mix proportions of both the cement and geopolymer composites are given in Table 2. A low AMF volume fraction of 0.75% is used to reinforce both cement and geopolymer composites. This volume fraction is selected to ensure uniform dispersion of AMF in the composites during mixing. For the preparation of cement composites, OPC and sand were dry-mixed initially for three minutes with a ratio of 1:0.5. After that, AMFs were added, and the mixing was further continued for another three minutes to allow for uniform dispersion of fibres. In the end, water was added to the mixture with a *w/c* ratio of 0.5, and the mixing was then continued for another five minutes.

For the preparation of geopolymer composites, alkali activators were prepared 24 h prior to mix to allow for the heat dissipation caused by the chemical reaction between sodium hydroxide (NaOH) and sodium silicate (Na_2SiO_3) solutions. For the sample preparation, similar to the cement composite samples, class F fly ash was first mixed with the silica sand for two minutes followed by the slow addition of alkali activators with a binder to alkali activator ratio of 1:0.5. This mixing was continued for three minutes followed by the addition of AMF to the wet mix and the mixing was then continued until the fibres were all well dispersed.

Table 2. Mix proportions of cement and geopolymer composites.

Composite	Binder		Sand	Alkali Activator (Weight)		Water (Weight)	AMF (Volume)
	Cement	Fly Ash		NaOH	Na ₂ SiO ₃		
CC	1	-	0.5	-	-	0.5	-
AMF-CC	1	-	0.5	-	-	0.5	0.75%
GC	-	1	0.5	0.15	0.35	-	-
AMF-GC	-	1	0.5	0.15	0.35	-	0.75%

After the mixing, the composites were cast in respective molds for compression and flexural strength tests followed by their compaction and removal of air voids by placing them on vibrating tables for about 1–2 min. The cement composite molds were then cured at room temperature ($28\text{ }^{\circ}\text{C} \pm 3\text{ }^{\circ}\text{C}$), whereas the geopolymer composite molds were first cured in the oven at $70\text{ }^{\circ}\text{C}$ for 24 h. After 24 h of curing and demolding, the cement composite samples were cured in water and the geopolymer composite samples were cured at room temperature ($28\text{ }^{\circ}\text{C} \pm 3\text{ }^{\circ}\text{C}$) for 28 days.

2.2.2. Exposure to Elevated Temperatures

After 28 days of curing and drying of the composites, all specimens were heated at designated elevated temperatures in the electric kiln with a maximum temperature rating of $1200\text{ }^{\circ}\text{C}$. The samples were heated to four different temperature ranges of $200\text{ }^{\circ}\text{C}$, $400\text{ }^{\circ}\text{C}$, $600\text{ }^{\circ}\text{C}$, and $800\text{ }^{\circ}\text{C}$. The heating rate for all the samples was kept at $5\text{ }^{\circ}\text{C}$ per minute, as recommended by RILEM [43], until the desired temperature was attained. For measuring the ambient temperature in the kiln and temperature on the surface of the samples, two “type K” thermocouples were used which were connected to the data logger. After attaining the desired temperature, the samples were kept in the kiln for an additional 120 min to ensure that the core temperature also attained the desired temperature. After heating, the samples were left inside the kiln, as shown in Figure 2, overnight to cool in ambient temperature inside the laboratory and then weighed to determine any weight loss.

**Figure 2.** Flexure specimens in kiln after heating.

Overall, four different types of specimens were cast which were unreinforced cement composite (CC), AMF reinforced cement composite (AMF-CC), unreinforced geopolymer composite (GC), and AMF reinforced geopolymer composite (AMF-GC). For each type of composite, three specimens were cast for each temperature of ambient, $200\text{ }^{\circ}\text{C}$, $400\text{ }^{\circ}\text{C}$, $600\text{ }^{\circ}\text{C}$, and $800\text{ }^{\circ}\text{C}$.

2.3. Experimental Test-Setup

For the compressive strength tests, 50 mm cubes were prepared according to Australian standard AS1012.9:20210 [44], and for the flexural strength tests, plate specimens with $400 \times 40 \times 15\text{ mm}$ dimensions were prepared. Thin plate specimens are widely used by various researchers in short fibre reinforced cementitious composites. The specimen size used in flexural specimens in this study is very similar to that used by others, including the authors in a previous study [18]. The compression strength test was conducted as per AS 1012.9:2014 [44] using a 300 kN capacity Shimadzu universal testing machine, and the flexural strength test was conducted on a 50 kN capacity universal testing machine. For the

flexural strength test, 3-point loading with a central point load was applied on the plate specimens with a clear span of 300 mm and a loading rate of 0.5 mm/min. A linear voltage displacement transducer (LVDT) was placed at the center of the plate specimen to measure the deflections in the flexural test.

3. Results and Discussions

3.1. Post-Heating Physical Properties

When exposed to elevated temperatures, both the cement and geopolymer composites exhibited mass loss. The mass of the cube samples before and after heating were measured, and the average values are presented in Figure 3. From this table, it can be seen that an increase in the exposure temperature leads to greater mass loss, and the maximum mass loss was observed in samples heated to 800 °C. Overall, the mass loss in geopolymer composites was lower than that of the cement composites, especially at 800 °C where the average mass loss in geopolymer composites was 11% versus 23% in cement composites. The mass loss of 11% in the geopolymer composites is similar to the results of Hosan et al. [41], who obtained similar values for un-reinforced geopolymer composites.

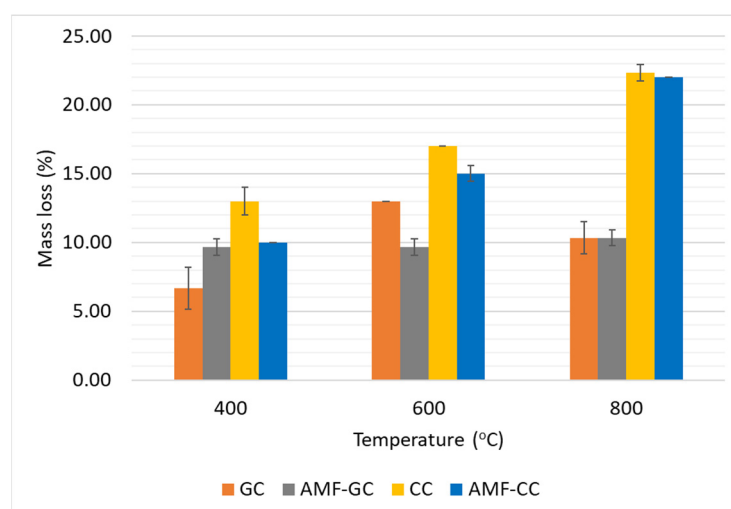


Figure 3. Mass loss of cement and geopolymer composites at elevated temperatures.

The cracking behavior of the cement and geopolymer composites at ambient and elevated temperatures is presented in Figure 4. For both the unreinforced and reinforced cement composites (Figure 4a), there was no significant cracking at 200 °C and 400 °C. However, on further increasing the temperature, cracks started appearing on the surface. For the unreinforced cement composites at 600 °C, a significant number of cracks can be seen on the surface, whereas only a small number of cracks can be seen on reinforced cement composite specimens. For the geopolymer composites (Figure 4b), on the other hand, none of the specimens cracked which is also exhibited by small amounts of mass loss in these samples (Figure 3).

Also, the color of the specimens changed to slightly reddish at elevated temperatures. For the cement composites, this color change started appearing at 400 °C while for the geopolymer composites, this color shift started occurring at 600 °C. The cracking behavior observed is similar to the behavior observed by Lu and Anson [45] and Shaikh and Hosan [46]. For the cement composites, Lu and Anson [45] found that the unreinforced cement composites started cracking at 400 °C while the reinforced cement composites started cracking at 600 °C and the cracking became severe with the further increase to 800 °C. Shaikh and Hosan [46] also observed that the cracking in steel fibre reinforced cement composites (SFRC) started occurring at 600 °C and became severe at 800 °C while the steel fibre reinforced geopolymer composite showed no sign of cracking up until 800 °C.

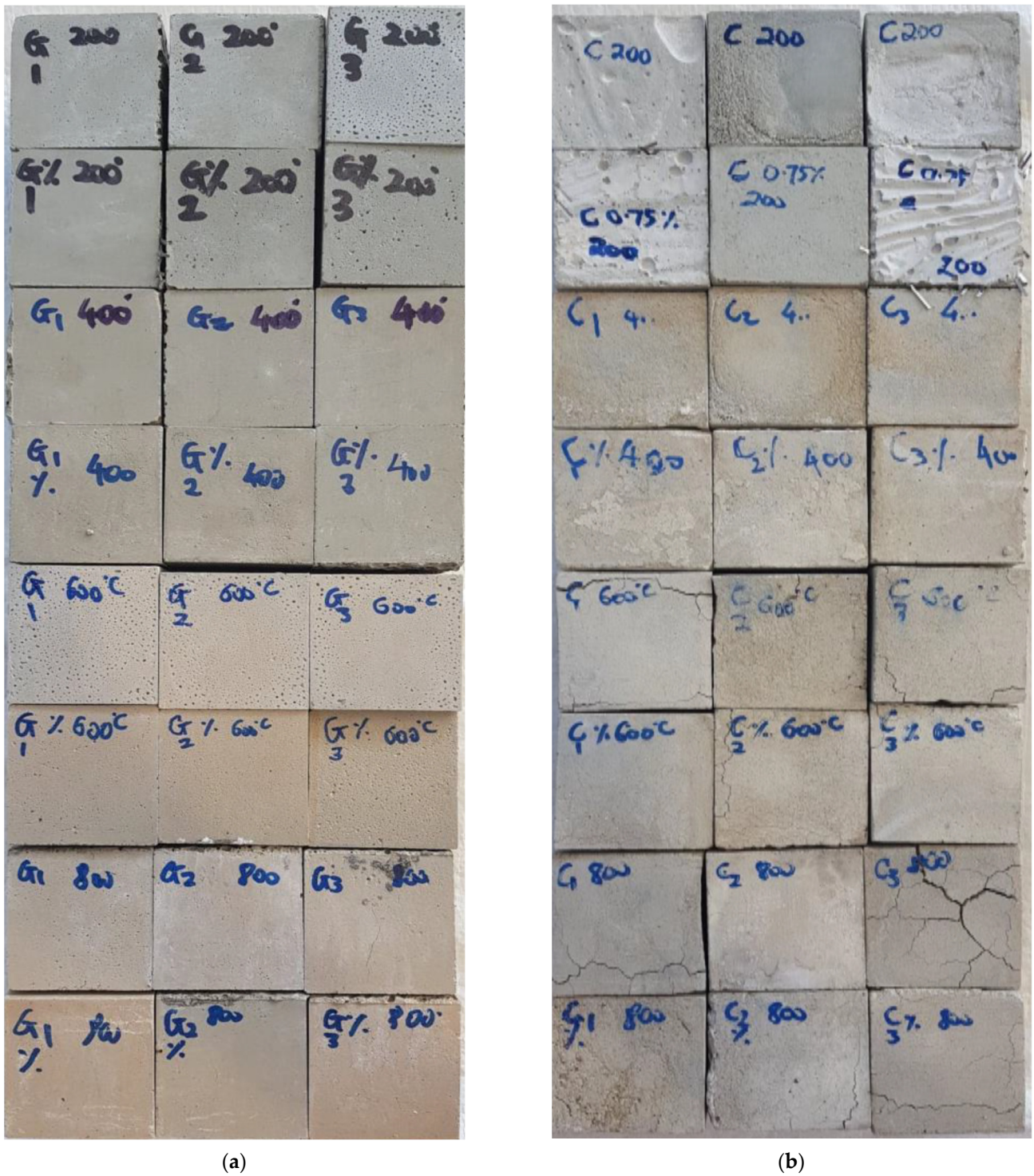


Figure 4. Cracking behavior of composites at elevated temperatures (a) Cement composites (b) Geopolymer composites.

3.2. Residual Compressive Strength

The compressive strength test results of both cement and geopolymer composites reinforced by amorphous metallic fibres are presented in Figure 5. At the initial rise in temperature from 28 °C to 200 °C, cement and geopolymer composites exhibited different behavior as the strength of reinforced cement composites reduced from 66 MPa to 58 MPa while the strength of reinforced geopolymer composites increased from 69 MPa to 76 MPa.

However, after 200 °C, both composites exhibited similar behavior as their strength reduced with the increase in temperature. The compressive strength of the reinforced cement composites was reduced to 50 MPa, 29 MPa, and 29 MPa at 400 °C, 600 °C, and 800 °C respectively. The corresponding reduced compressive strengths of reinforced geopolymer composites were 51 MPa, 36 MPa, and 31 MPa, respectively. The percentage reduction in compressive strength of both the samples is presented Figure 6 which also shows an initial increase in compressive strength of geopolymer concrete (by 10%) at 200 °C and then further reduction by 26%, 50% and 56% at 400 °C, 600 °C, and 800 °C respectively.

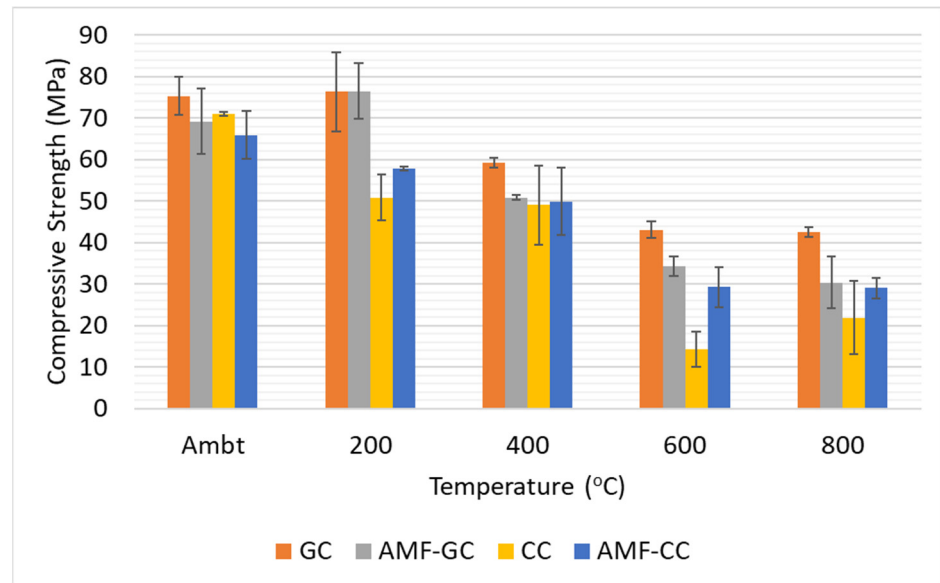


Figure 5. Compressive strength of unreinforced and AMF reinforced cement and geopolymer composites.

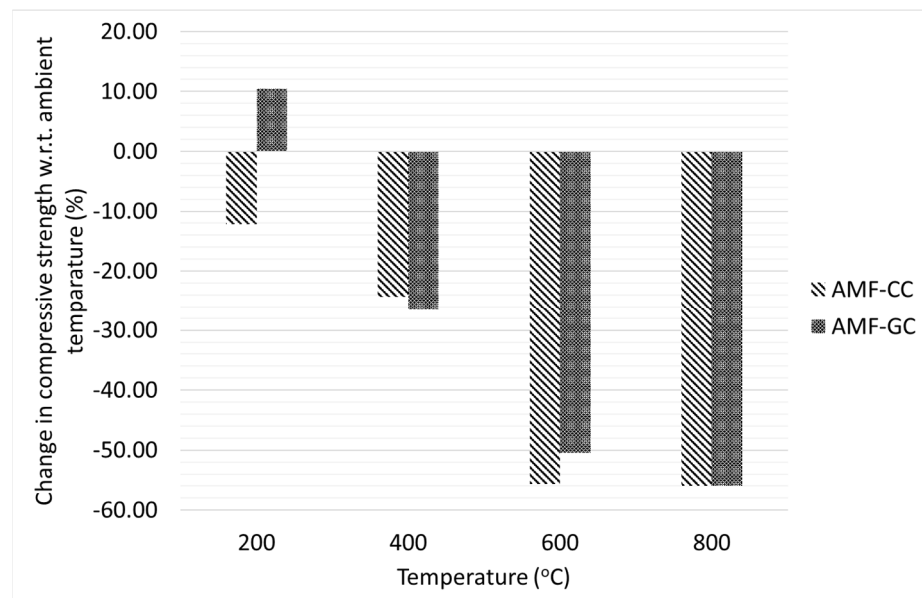


Figure 6. Change in compressive strength of AMF reinforced cement and geopolymer composite at elevated temperatures.

Similar results in the reduction of residual compressive strength of fibre-reinforced cement and geopolymer composites at elevated temperatures have been obtained by previous researchers. As the composite is heated, cracks begin to appear and expand

gradually due to a number of reasons including hydration and dehydration of C-S-H in the matrix, thermal incompatibility of aggregates and cement, and pore pressure generated by water in the pores [47,48]. The addition of fibres bridges the cracks and the high melting point of fibres can result in a good performance at elevated temperatures [49]. For the SFRCs, Poon et al. [50] reported residual strengths of 50% and 25% at 600 °C, and 800 °C respectively. In another study, Chen and Liu [51] reported residual strengths of 90%, 60%, and 38% at the temperatures of 400 °C, 600 °C, and 800 °C respectively. Bezerra et al. [52] also reported 59% residual strength of SFRC at the temperature of 500 °C. A comparison of SFRC results at similar elevated temperatures to that of the present study is presented in Table 3. From this table, it can be seen that AMF reinforced cement composite possesses good residual strength at elevated temperatures which is comparable to that of the SFRCs. This table also indicates that the SFRCs with higher fibre ratios possess higher residual strength which is consistent with the conclusion of Chen et al. [53] that the increase in fibre ratio has a direct relation with the residual strength. Another interesting observation is the residual strength of AMF reinforced concrete at the temperature of 800 °C, where it still has 44% residual compressive strength which is higher than that of the corresponding SFRCs except Ismail et al. [54], who used high strength concrete.

Table 3. Comparison of residual compressive strengths of steel fibre reinforced composites at elevated temperatures.

Study	Fibre Content	Strength	Temperature (°C)				
			Ambient	200	400	600	800
Present study	0.75%	Compressive strength (MPa)	66	58	50	29	29
		Residual strength (%)		88	76	44	44
Shaikh and Hosan [46]	0.75%	Compressive strength (MPa)	48	42	40	27	20
		Residual strength (%)		88	83	56	42
Lau and Anson [45]	1%	Compressive strength (MPa)	45	34	30	20	12
		Residual strength (%)		76	67	44	27
		Compressive strength (MPa)	60	48	40	33	17
		Residual strength (%)		80	67	55	28
Colombo et al. [55]	2%	Compressive strength (MPa)	75	62	59	47	-
		Residual strength (%)		83	78	63	-
Li et al. [56]	1%	Compressive strength (MPa)	40	38	48	29	8
		Residual strength (%)		95	120	73	20
	2%	Compressive strength (MPa)	37	36	40	34	7
		Residual strength (%)		97	108	92	19
Ismail et al. [54]	0.50%	Compressive strength (MPa)	52	49	50	42	38
		Residual strength (%)		95	97	81	74

For the steel reinforced geopolymer composite, Shaikh and Hosan [46] evaluated the compressive strength of sodium activator-based geopolymer composites reinforced with the same steel fibres ratio of 0.75%. They obtained the residual compressive strength of 128%, 111%, 89%, and 59% at the temperatures of 200 °C, 400 °C, 600 °C, and 800 °C respectively. These values are relatively higher than those achieved for AMF reinforced geopolymer composites reported in this study which are probably due to added advantage of geopolymer composites with steel fibres. Since the number of research studies on AMF reinforced geopolymer composites is not enough, therefore, more experimental data is required to reach any conclusion.

3.3. Residual Flexural Strength

Load and mid-span deflection behaviour of the unreinforced and AMF reinforced cement and geopolymer composites are presented in Figures 7 and 8, respectively. At the same temperature for all composites, it can be seen that the flexural load capacity increases

when the composites are reinforced with AMFs and the ductility of the specimens also improves significantly as exhibited by the plateau of load-displacement curves after the initiation of cracks. The average load capacities of cement composites at ambient, 200 °C, and 400 °C are improved by 90%, 67%, and 90% respectively when reinforced with AMF. Similarly, the average load capacities of geopolymer composites at ambient, 200 °C, 400 °C, 600 °C, and 800 °C are improved by 7%, 8%, 49%, 122%, and 102% respectively when reinforced with AMF.

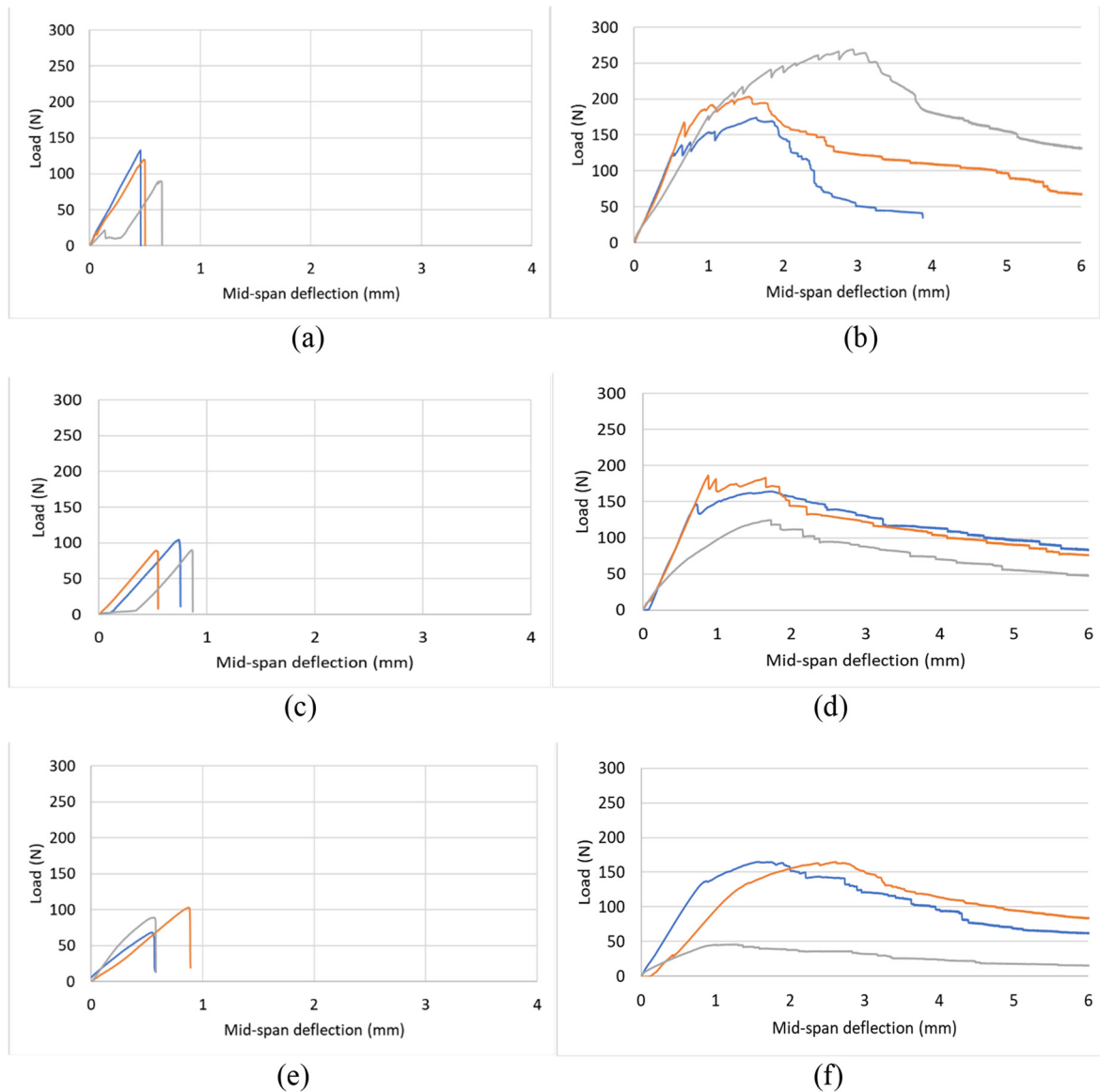


Figure 7. Flexural load vs. midspan deflection (a) UCC at ambient temperature (28 °C) (b) RCC at ambient temperature (28 °C) (c) UCC at 200 °C (d) RCC at 200 °C (e) UCC at 400 °C (f) RCC at 400 °C.

The improvement in ductility of the composites with AMF reinforcement is attributed to the friction bond between AMF fibres and the matrix of the composites. After the formation of the first crack under bending deformation, if the friction between AMF fibres and the matrix is greater than the applied load, then more cracks are formed and the specimen keeps on resisting more loads with increased deformations. This resistance of higher loads with higher deformations leads to deflection hardening behavior and the ductility of the member is significantly improved.

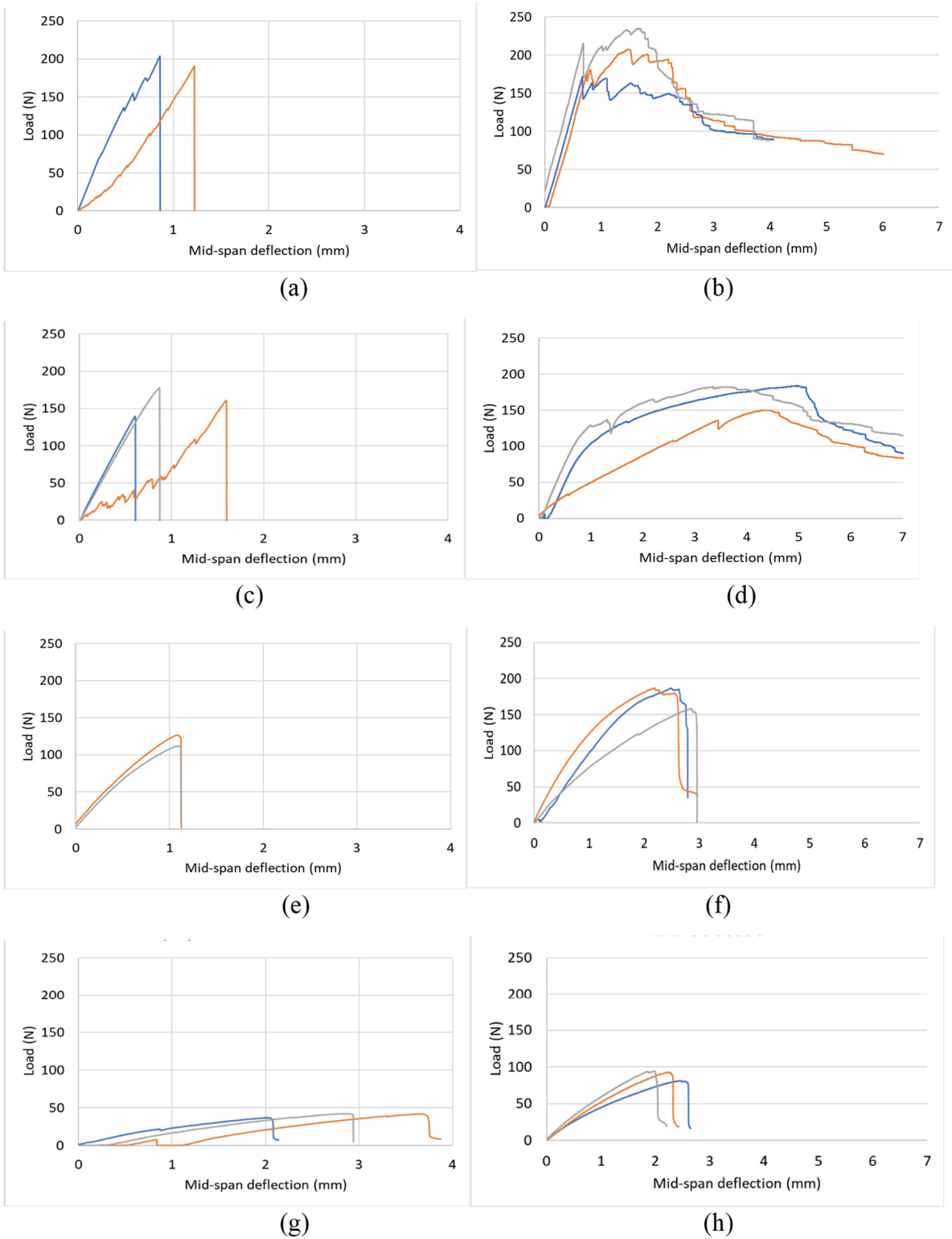


Figure 8. Cont.

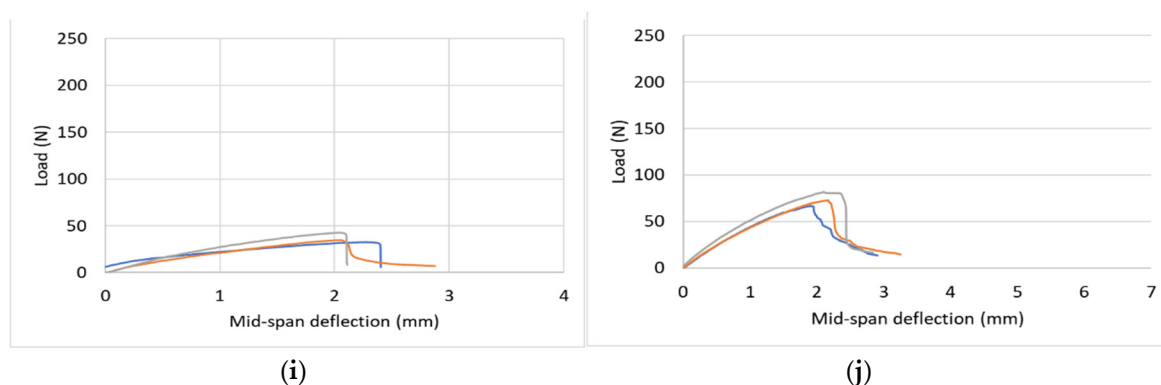


Figure 8. Flexural load vs. midspan deflection (a) UGC at ambient temperature (28 °C) (b) RGC at ambient temperature (28 °C) (c) UGC at 200 °C (d) RGC at 200 °C (e) UGC at 400 °C (f) RGC at 400 °C (g) UGC at 600 °C (h) RGC at 600 °C (i) UGC at 800 °C (j) RGC at 800 °C.

For the cement composites, the increase in temperature has adverse effects on the load capacity of the members as the load capacity decreased with the increase in temperature (Figure 7). Also, the cement composites which were heated at temperatures higher than 400 °C could not be tested as the specimens completely deteriorated. The average load capacities were reduced by 17% and 24% at 200 °C and 400 °C respectively. The corresponding decrease in load capacities of reinforced cement composites was 26% and 24%. Similar behavior was observed in geopolymer composites as the load capacity decreased with increasing temperature except at 400 °C (Figure 8e,f) at which there was an increase in the capacity as compared to the capacity at 200 °C (Figure 8c,d). The average load capacities of the unreinforced geopolymer composites were reduced by 19%, 40%, 80%, and 82% at 200 °C, 400 °C, 600 °C, and 800 °C respectively. The corresponding decrease in load capacities of AMF reinforced geopolymer composites were 17%, 14%, 56%, and 64% respectively. Significant reduction in the ductility was observed in the geopolymer composites at elevated temperatures as the deformation at higher loads reduced drastically even as compared to the ones for cement composite at 400 °C (Figure 7e,f). Both the unreinforced and reinforced geopolymer composites exhibited brittle failure at 600 °C (Figure 8g,h) and 800 °C (Figure 8i,j). Similar behavior of reduced deformations at peak loads for geopolymer composites was observed by Shaikh et al. [18] in heat-cured geopolymer composites as compared to cement composites.

The flexural strengths and change in flexural strengths of reinforced cement and reinforced geopolymer composites at elevated temperatures are presented in Figures 9 and 10, respectively. At the ambient temperature, reinforced cement composites had a slightly higher flexural strength than their counterpart geopolymer composites. When the temperature was increased to 200 °C (Figure 9), the flexural strength of the cement composites reduced from 10.8 MPa to 7.90 MPa, and the flexural strength of the reinforced geopolymer composites reduced from 10.2 MPa to 8.6 MPa, surpassing the flexural strength of cement composite. As the temperature increased to 400 °C, the flexural strength of both the cement and geopolymer composites slightly improved to 8.1 MPa and 8.8 MPa respectively. The cement composites beyond 400 °C could not be tested and the flexural strength of geopolymer composites was reduced to 4.4 MPa and 3.6 MPa at 600 °C and 800 °C respectively. The residual strength of the cement composites at 200 °C and 400 °C was 74% and 76% respectively whereas the residual strength of the geopolymer composites at 200 °C, 400 °C, 600 °C, and 800 °C was 84%, 86%, 44%, and 36% respectively (Figure 10).

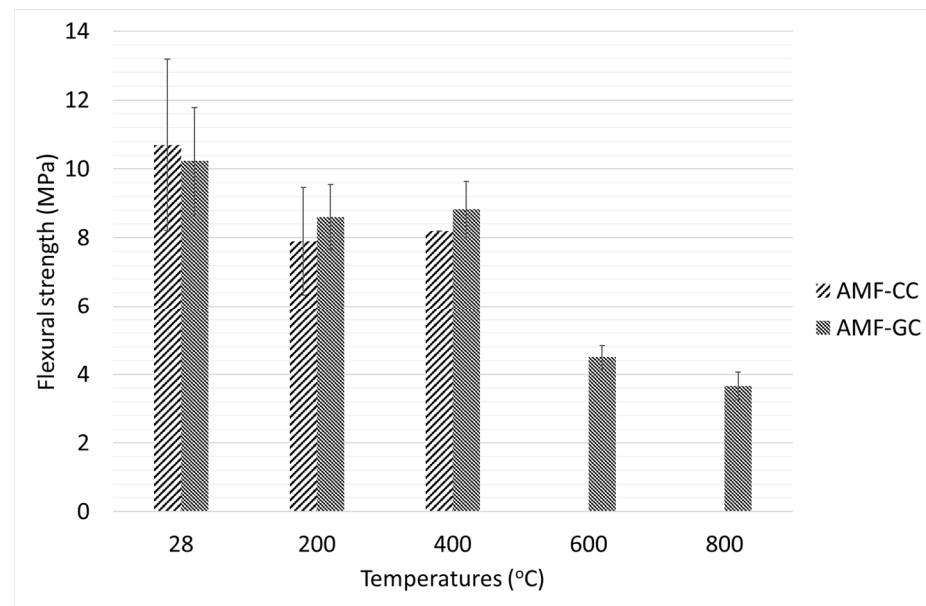


Figure 9. Flexural strength of AMF reinforced cement and geopolymer concrete.

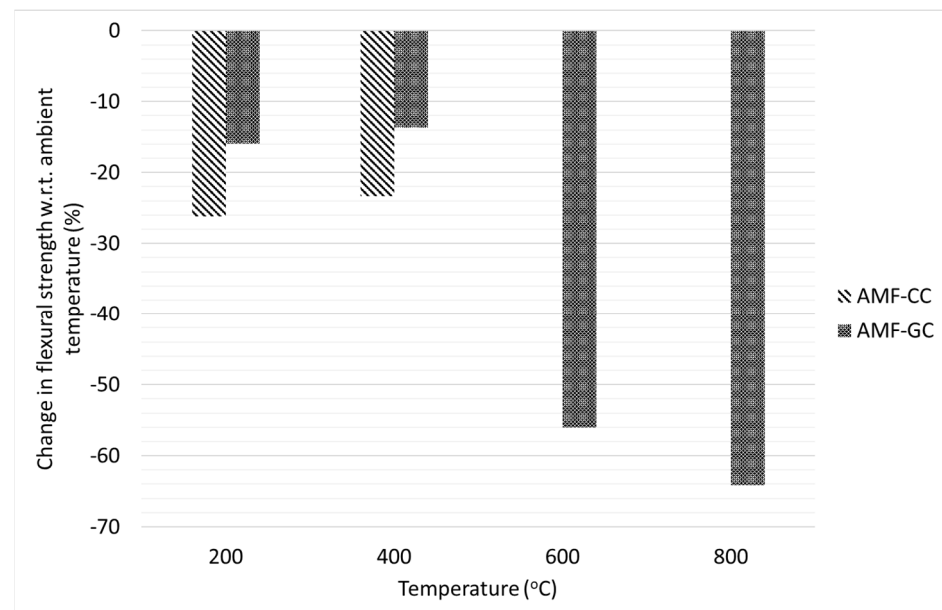


Figure 10. Change in flexural strength of AMF reinforced cement and geopolymer concrete at elevated temperature.

A comparison of residual flexural strength of AMF reinforced cement composites with SFRCs at similar elevated temperatures is given in Table 4. For all the composites, it can be seen that the residual flexural strength decreases with an increase in temperatures, and the composites with higher fibre ratios possess higher residual strengths at the elevated temperature of 200 °C. Interestingly, at 400 °C, the residual flexural strength of AMF-CC with a lower fibre ratio was higher than the other SF-GC with higher fibre ratios. A similar decrease in the residual flexural strength at different elevated temperatures was also evaluated by Pliya et al. [57], Choumanidis et al. [58], and Jameran et al. [59]. At temperatures higher than 400 °C, the AMF-CC could not be tested whereas the SFRCs with higher steel fibre ratio possess relatively good strength even at higher temperatures. To draw the comparison at these temperatures, further research is needed with higher ratios of AMF in composites.

Table 4. Comparison of residual flexural strengths of steel fibre reinforced composites at elevated temperatures.

Study	Fibre Content	Strength	Temperature (°C)				
			Ambient	200	400	600	800
Present study	0.75%	Flexural strength (MPa)	10.8	7.9	8.1	-	-
		Residual strength (%)		73	75	-	-
Lau and Anson [45]	1%	Flexural strength (MPa)	6	5	3	1.2	0.1
		Residual strength (%)		83	50	20	2
		Flexural strength (MPa)	8	7	4	2.8	1
		Residual strength (%)		88	50	35	13
Colombo et al. [55]	2%	Flexural strength (MPa)	4	3	2	2	-
		Residual strength (%)		84	45	39	-

The toughness of the reinforced cement and geopolymers composites was also calculated and the average results are presented in Figure 11. Toughness is an important parameter to assess the energy absorption capacity of a member and is calculated by the area under the load-deflection curve up to a given deflection. In Figure 11 the toughness presented has been calculated using the area under the load-deflection curves until the point of peak load and the values given are the average of 3 specimens. Overall, the toughness of AMF reinforced geopolymer composites was higher than that of the cement composites and these toughness values increased up to 400 °C. The toughness increased slightly for cement composites whereas there was a sudden jump in the toughness of reinforced geopolymer composites at 400 °C as the toughness increased by 230% as compared to the toughness at ambient temperature. After 400 °C, there was a sharp decrease in the toughness of reinforced geopolymer composite, however, the toughness at 800 °C was still higher in reinforced geopolymer composite than the toughness at ambient temperature. The toughness results are also consistent with previous research studied on fracture toughness and fracture energy [60,61], which found that the fracture energy of the composites increases gradually as the temperature increases from 25 °C to 400 °C. As compared to the sharp crack development at room temperature, the crack development and propagation at higher temperatures are quite complex and this complexity is exacerbated by the inclusion of fibres [49].

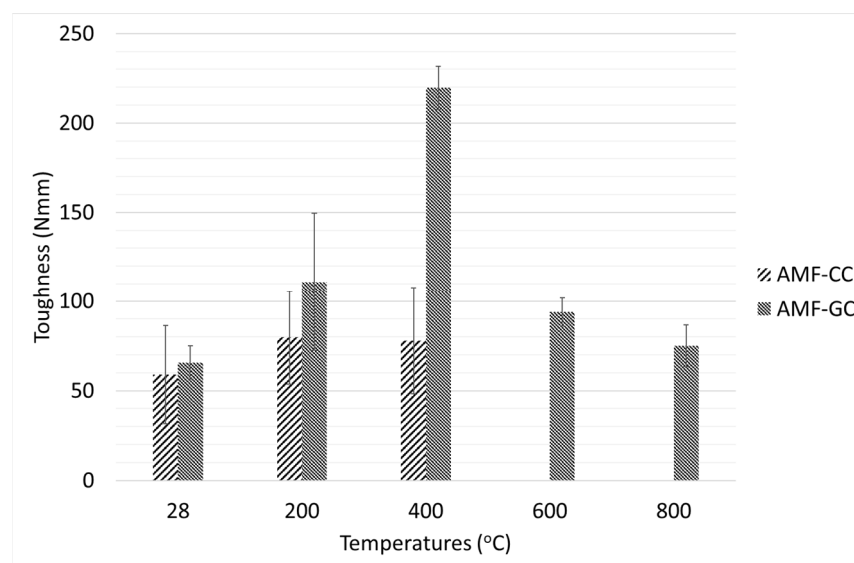


Figure 11. Toughness of AMF reinforced cement and geopolymer concrete at elevated temperature.

3.4. Microstructure Analysis of Cement and Geopolymer Composites

The scanning electron microscope (SEM) images of reinforced cement composites and geopolymer composites are presented in Figures 12 and 13, respectively. For the AMF fibres at ambient temperatures in the cement composite (Figure 12a) and in the geopolymer composite (Figure 13a), it can be seen that the surface of the fibre is relatively rough and the matrix is also present on the surface of the fibre. For the cement composite (this matrix is smaller in amount than the geopolymer composite which explains the reason for the higher compressive and flexural strengths of geopolymer composites than the cement composites. As the temperature increases, the amount of matrix on the fibres decreases. For the cement composites at 800 °C (Figure 12b), it can be seen that the amount of matrix on the fibres is negligible which resulted in significant cracking in lower residual flexural strength of reinforced composites. However, for the reinforced geopolymer composite at 800 °C, the surface of the fibre is relatively rough than that of the cement composite and a higher amount of geopolymer matrix is present on the surface of the fibre. This rough surface of the fibre and higher amount of matrix explains the reason for negligible cracking in the geopolymer composite specimens and higher residual compressive and flexural strength of these composites.

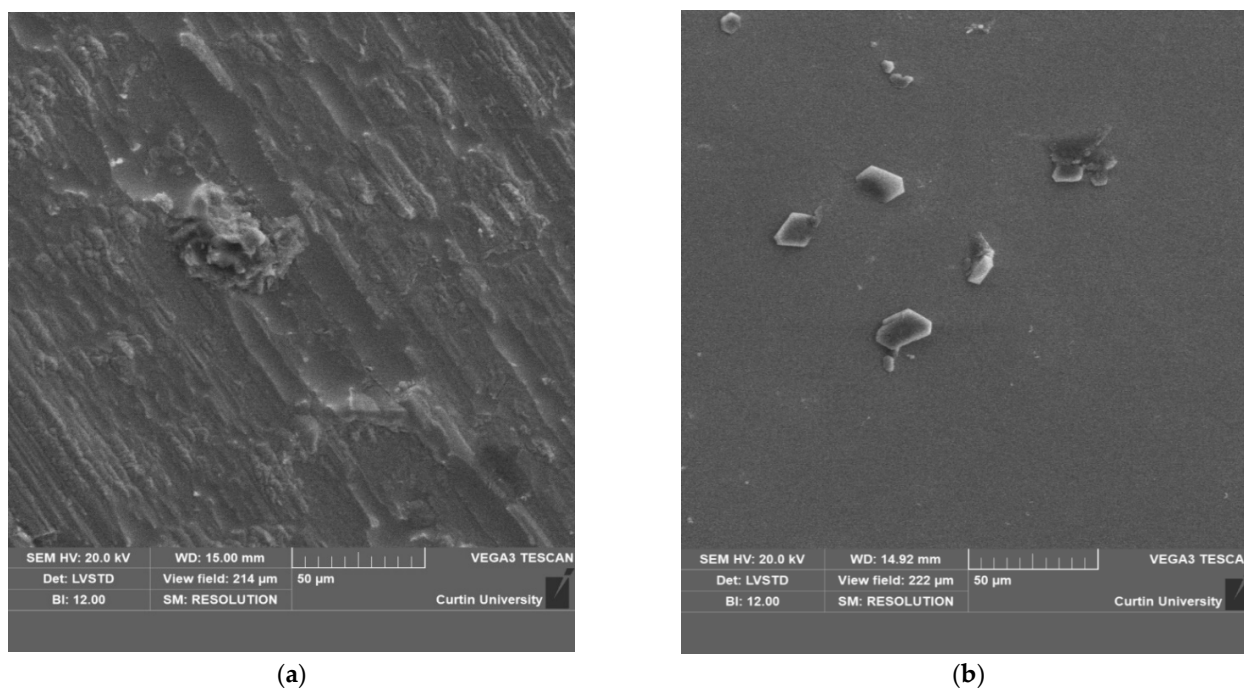


Figure 12. SEM images of surface of AMF fibers in cement composites at (a) ambient temperature (b) 800 °C.

It has been well established that the increase in temperature negatively affects the properties of composites, however, geopolymer-based composites perform better than cement-based composites [62,63]. The C-S-H and CH products in cement composites are affected more at higher temperatures along with an increase in the porosity of the cement composites [45] which results in faster degradation of matrix-fibre bond and reduction of fibre efficiency [64]. For the geopolymer composites, the (N-A-S-H) gel has higher stability at elevated temperatures and the presence of mullite, a stable crystalline phase of $Al_2O_3-SiO_2$ which possesses high thermal stability, also contributes to superior mechanical properties at elevated temperatures [41]. Shaikh and Hosan [46] conducted SEM image analysis of steel fibres in cement and geopolymer composites and found that the steel fibres in the cement composites showed surface layers peeling at 600 °C whereas no such deterioration of the same fibres was observed in geopolymer composites even at 800 °C. Therefore, the embedment of fibres in the geopolymer composites helps in the retention of fibre properties even at elevated temperatures.

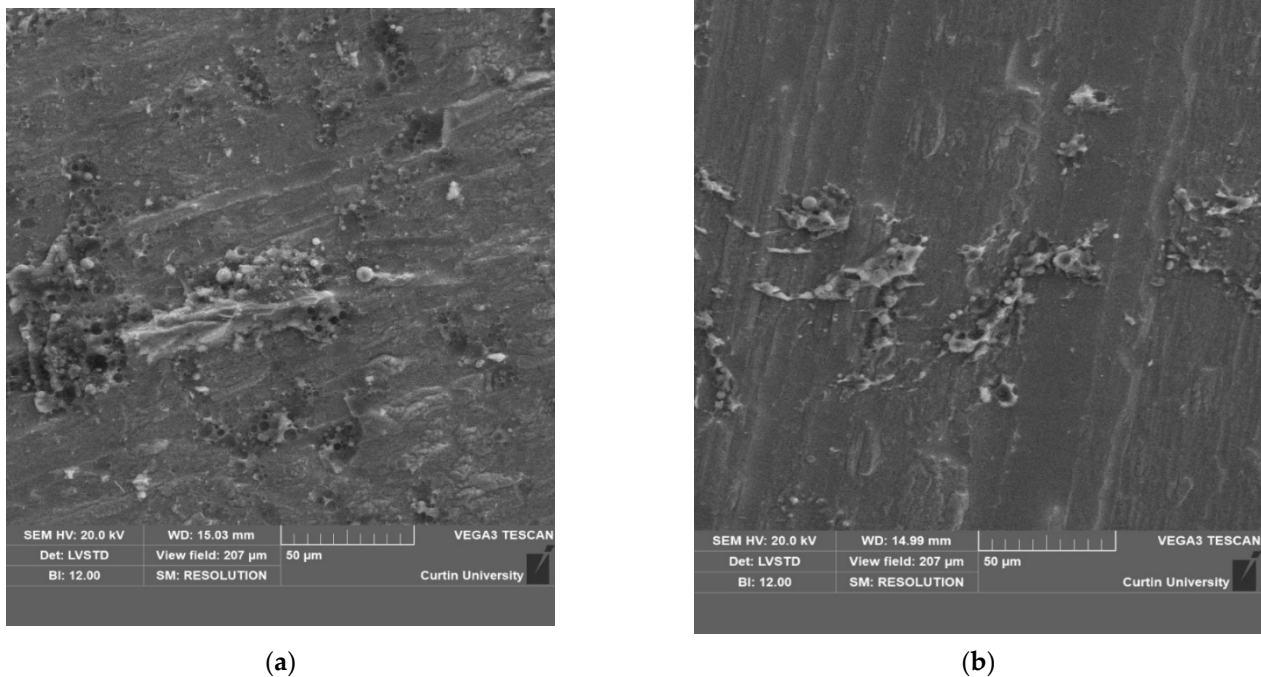


Figure 13. SEM images of surface of AMF fibers in geopolymer composites at (a) ambient temperature (b) 800 °C.

4. Conclusions

In this research study, experimental tests were conducted on unreinforced and amorphous metallic fibre (AMF) reinforced cement and geopolymer composites to assess their residual behavior after exposed to elevated temperatures. The following conclusions are drawn based on the research study:

- The average mass loss in unreinforced and AMF reinforced cement composites was higher than their geopolymer counterparts at all elevated temperatures.
- Cracking was negligible in both the AMF reinforced cement and geopolymer composites up to 400 °C. At 600 °C and 800 °C temperatures the AMF reinforced geopolymer composites exhibited no cracking.
- The compressive strength of AMF reinforced geopolymer composites was higher than that of cement composites at all temperature levels. The residual compressive strength of reinforced cement composites at 200 °C, 400 °C, 600 °C, and 800 °C was 88%, 76%, 44%, and 45% to that of the strength at ambient temperature. The corresponding residual strength of reinforced geopolymer composites was 110%, 74%, 49%, 45%.
- Similar to the compressive strength, the flexural strength of the composites also reduced with increasing temperature and the flexural strength of the AMF reinforced geopolymer composites was higher than that of cement composites at all elevated temperatures. The residual flexural strengths of AMF reinforced cement composites at 200 °C, 400 °C, 600 °C were 76%, 78% respectively, while the residual flexural strengths of AMF reinforced geopolymer composites at 200 °C, 400 °C, 600 °C, and 800 °C were 80%, 81%, 43%, and 45% to that of the strength at ambient temperature.
- Scanning electron microscopic images also showed increased deterioration of cement composites at higher temperatures than the geopolymer composites. At the temperature of 800 °C, a negligible amount of cement matrix was present on the fibres which results in significant cracking and lower residual strengths than the geopolymer composites in which a higher amount of geopolymer matrix was still present on the fibres. The superior fire resisting properties of the geopolymer matrix also help in the retention of the fibre integrity at elevated temperatures.

Author Contributions: Conceptualization, F.U.A.S.; methodology, F.U.A.S.; formal analysis, A.U.R.D. and N.S.K.; investigation, N.S.K.; resources, F.U.A.S.; writing—original draft preparation, A.U.R.D.; writing—review and editing, F.U.A.S.; supervision, F.U.A.S.; project administration, F.U.A.S. All authors have read and agreed to the published version of the manuscript.

Funding: This research received no external funding.

Data Availability Statement: Data is available upon request to corresponding author.

Conflicts of Interest: The authors declare no conflict of interest.

References

1. Huntzinger, D.N.; Eatmon, T.D. A life-cycle assessment of Portland cement manufacturing: Comparing the traditional process with alternative technologies. *J. Clean. Prod.* **2009**, *17*, 668–675. [\[CrossRef\]](#)
2. Davidovits, J. Soft mineralogy and geopolymers. In Proceedings of the Geopolymer 88 International Conference, the Université de Technologie, Compiègne, France, 1–3 June 1988; Volume 88, pp. 49–56.
3. Davidovits, J. High-alkali cements for 21st century concretes. *Spec. Publ.* **1994**, *144*, 383–398.
4. Al-Mashhadani, M.M.; Canpolat, O.; Aygörmez, Y.; Uysal, M.; Erdem, S. Mechanical and microstructural characterization of fibre reinforced fly ash based geopolymer composites. *Constr. Build. Mater.* **2018**, *167*, 505–513. [\[CrossRef\]](#)
5. Li, Z.; Ding, Z.; Zhang, Y. Development of Sustainable Cementitious Materials. In Proceedings of the International Workshop on Sustainable Development and Concrete Technology, Beijing, China, 20–21 May 2004; pp. 55–76.
6. Duxson, P.; Provis, J.L.; Lukey, G.C.; Van Deventer, J.S.J. The role of inorganic polymer technology in the development of ‘green concrete’. *Cem. Concr. Res.* **2007**, *37*, 1590–1597. [\[CrossRef\]](#)
7. Huang, C.-H.; Lin, S.-K.; Chang, C.-S.; Chen, H.-J. Mix proportions and mechanical properties of concrete containing very high-volume of Class F fly ash. *Constr. Build. Mater.* **2013**, *46*, 71–78. [\[CrossRef\]](#)
8. Mehta, P.K. Pozzolanic and cementitious byproducts as mineral admixtures for concrete—a critical review. *Spec. Publ.* **1983**, *79*, 1–46.
9. Swanepoel, J.C.; Strydom, C.A. Utilisation of fly ash in a geopolymeric material. *Appl. Geochem.* **2002**, *17*, 1143–1148. [\[CrossRef\]](#)
10. Malhotra, V.M. Fly ash, slag, silica fume, and rice husk ash in concrete: A review. *Concr. Int.* **1993**, *15*, 23–28.
11. Olivia, M.; Nikraz, H. Properties of fly ash geopolymer concrete designed by Taguchi method. *Mater. Des.* **2012**, *36*, 191–198. [\[CrossRef\]](#)
12. Phoo-ngernkham, T.; Maegawa, A.; Mishima, N.; Hatanaka, S.; Chindapasirt, P. Effects of sodium hydroxide and sodium silicate solutions on compressive and shear bond strengths of FA–GBFS geopolymer. *Constr. Build. Mater.* **2015**, *91*, 1–8. [\[CrossRef\]](#)
13. Phoo-Ngernkham, T.; Sata, V.; Hanjitsuwan, S.; Riddtirud, C.; Hatanaka, S.; Chindapasirt, P. High calcium fly ash geopolymer mortar containing Portland cement for use as repair material. *Constr. Build. Mater.* **2015**, *98*, 482–488. [\[CrossRef\]](#)
14. Hardjito, D.; Wallah, S.E.; Sumajouw, D.M.J.; Rangan, B.V. On the development of fly ash-based geopolymer concrete. *Mater. J.* **2004**, *101*, 467–472.
15. Wallah, S.; Rangan, B.V. *Low-Calcium Fly Ash-based Geopolymer Concrete: Long-Term Properties*; Curtin University: Perth, WA, Australia, 2006.
16. Kong, D.L.Y.; Sanjayan, J.G. Effect of elevated temperatures on geopolymer paste, mortar and concrete. *Cem. Concr. Res.* **2010**, *40*, 334–339. [\[CrossRef\]](#)
17. Sarker, P.K. Analysis of geopolymer concrete columns. *Mater. Struct.* **2009**, *42*, 715–724. [\[CrossRef\]](#)
18. Shaikh, F.U.A.; Singh, A.S.D.; Pandra, A. Mechanical Properties of Amorphous Metallic Fibre-Reinforced Geopolymer Composites. *J. Mater. Civ. Eng.* **2022**, *34*, 1–14. [\[CrossRef\]](#)
19. Choi, S.-J.; Hong, B.-T.; Lee, S.-J.; Won, J.-P. Shrinkage and corrosion resistance of amorphous metallic-fibre-reinforced cement composites. *Compos. Struct.* **2014**, *107*, 537–543. [\[CrossRef\]](#)
20. Yang, J.-M.; Shin, H.-O.; Yoo, D.-Y. Benefits of using amorphous metallic fibres in concrete pavement for long-term performance. *Arch. Civ. Mech. Eng.* **2017**, *17*, 750–760. [\[CrossRef\]](#)
21. Kim, H.; Kim, G.; Nam, J.; Kim, J.; Han, S.; Lee, S. Static mechanical properties and impact resistance of amorphous metallic fibre-reinforced concrete. *Compos. Struct.* **2015**, *134*, 831–844. [\[CrossRef\]](#)
22. Choi, K.-K.; Ku, D.-O. Flexural behaviour of amorphous metal-fibre-reinforced concrete. *Proc. Inst. Civ. Eng. Build.* **2015**, *168*, 15–25. [\[CrossRef\]](#)
23. Shaikh, F.U.A. Pullout behavior of hook end steel fibres in geopolymers. *J. Mater. Civ. Eng.* **2019**, *31*, 4019068. [\[CrossRef\]](#)
24. Khan, M.Z.N.; Shaikh, F.U.A.; Hao, Y.; Hao, H. Effects of curing conditions and sand-to-binder ratios on compressive strength development of fly ash geopolymer. *J. Mater. Civ. Eng.* **2018**, *30*, 4017267. [\[CrossRef\]](#)
25. Khan, M.Z.N.; Hao, Y.; Hao, H. Synthesis of high strength ambient cured geopolymer composite by using low calcium fly ash. *Constr. Build. Mater.* **2016**, *125*, 809–820. [\[CrossRef\]](#)
26. Cheng, T.-W.; Chiu, J.P. Fire-resistant geopolymer produced by granulated blast furnace slag. *Miner. Eng.* **2003**, *16*, 205–210. [\[CrossRef\]](#)

27. Barbosa, V.F.F.; MacKenzie, K.J.D. Synthesis and thermal behaviour of potassium sialate geopolymers. *Mater. Lett.* **2003**, *57*, 1477–1482. [[CrossRef](#)]
28. Barbosa, V.F.F.; MacKenzie, K.J.D. Thermal behaviour of inorganic geopolymers and composites derived from sodium polysialate. *Mater. Res. Bull.* **2003**, *38*, 319–331. [[CrossRef](#)]
29. Buchwald, A.; Hohmann, M.; Kaps, C.; Bettzieche, H.; Kühnert, J.-T. Stabilised foam clay material with high performance thermal insulation properties. *CFI (Ceram. Forum Int. Ber. DKG)* **2004**, *81*, E39–E42.
30. Rickard, W.D.A.; Vickers, L.; Van Riessen, A. Performance of fibre reinforced, low density metakaolin geopolymers under simulated fire conditions. *Appl. Clay Sci.* **2013**, *73*, 71–77. [[CrossRef](#)]
31. Choi, Y.C.; Park, B. Effects of high-temperature exposure on fractal dimension of fly ash-based geopolymer composites. *J. Mater. Res. Technol.* **2020**, *9*, 7655–7668. [[CrossRef](#)]
32. Rickard, W.D.A.; Temuujin, J.; van Riessen, A. Thermal analysis of geopolymer pastes synthesised from five fly ashes of variable composition. *J. Non. Cryst. Solids* **2012**, *358*, 1830–1839. [[CrossRef](#)]
33. Abdulkareem, O.A.; Al Bakri, A.M.M.; Kamarudin, H.; Nizar, I.K.; Ala'eddin, A.S. Effects of elevated temperatures on the thermal behavior and mechanical performance of fly ash geopolymer paste, mortar and lightweight concrete. *Constr. Build. Mater.* **2014**, *50*, 377–387. [[CrossRef](#)]
34. Ranjbar, N.; Mehrali, M.; Alengaram, U.J.; Metselaar, H.S.C.; Jumaat, M.Z. Compressive strength and microstructural analysis of fly ash/palm oil fuel ash based geopolymer mortar under elevated temperatures. *Constr. Build. Mater.* **2014**, *65*, 114–121. [[CrossRef](#)]
35. Shaikh, F.U.A.; Vimonsatit, V. Compressive strength of fly-ash-based geopolymer concrete at elevated temperatures. *Fire Mater.* **2015**, *39*, 174–188. [[CrossRef](#)]
36. Kong, D.L.Y.; Sanjayan, J.G. Damage behavior of geopolymer composites exposed to elevated temperatures. *Cem. Concr. Compos.* **2008**, *30*, 986–991. [[CrossRef](#)]
37. Guerrieri, M.; Sanjayan, J.G. Behavior of combined fly ash/slag-based geopolymers when exposed to high temperatures. *Fire Mater. An Int. J.* **2010**, *34*, 163–175. [[CrossRef](#)]
38. Masi, G.; Rickard, W.D.A.; Bignozzi, M.C.; Van Riessen, A. The effect of organic and inorganic fibres on the mechanical and thermal properties of aluminate activated geopolymers. *Compos. Part B Eng.* **2015**, *76*, 218–228. [[CrossRef](#)]
39. Fiore, V.; Scalici, T.; Di Bella, G.; Valenza, A. A review on basalt fibre and its composites. *Compos. Part B Eng.* **2015**, *74*, 74–94. [[CrossRef](#)]
40. Welter, M.; Schmücker, M.; MacKenzie, K.J.D. Evolution of the fibre-matrix interactions in basalt-fibre-reinforced geopolymer-matrix composites after heating. *J. Ceram. Sci. Technol.* **2015**, *6*, 17–24.
41. Hosan, A.; Haque, S.; Shaikh, F. Compressive behaviour of sodium and potassium activators synthesized fly ash geopolymer at elevated temperatures: A comparative study. *J. Build. Eng.* **2016**, *8*, 123–130. [[CrossRef](#)]
42. Zhang, H.; Kodur, V.; Cao, L.; Qi, S. Fibre reinforced geopolymers for fire resistance applications. *Procedia Eng.* **2014**, *71*, 153–158. [[CrossRef](#)]
43. RILEM TC. 129-MHT: Test methods for mechanical properties of concrete at high temperatures. *Mater. Struct.* **1995**, *28*, 410–414.
44. AS 1012.9; Methods of Testing Concrete—Compressive Strength Tests—Concrete, Mortar and Grout Specimens. Standards Australia: Sydney, Australia, 2014.
45. Lau, A.; Anson, M. Effect of high temperatures on high performance steel fibre reinforced concrete. *Cem. Concr. Res.* **2006**, *36*, 1698–1707. [[CrossRef](#)]
46. Shaikh, F.U.A.; Hosan, A. Mechanical properties of steel fibre reinforced geopolymer concretes at elevated temperatures. *Constr. Build. Mater.* **2016**, *114*, 15–28. [[CrossRef](#)]
47. Dügenci, O.; Haktanir, T.; Altun, F. Experimental research for the effect of high temperature on the mechanical properties of steel fibre-reinforced concrete. *Constr. Build. Mater.* **2015**, *75*, 82–88. [[CrossRef](#)]
48. Khoury, G.A. Effect of fire on concrete and concrete structures. *Prog. Struct. Eng. Mater.* **2000**, *2*, 429–447. [[CrossRef](#)]
49. Zhang, P.; Kang, L.; Wang, J.; Guo, J.; Hu, S.; Ling, Y. Mechanical properties and explosive spalling behavior of steel-fibre-reinforced concrete exposed to high temperature—A review. *Appl. Sci.* **2020**, *10*, 2324. [[CrossRef](#)]
50. Poon, C.S.; Shui, Z.H.; Lam, L. Compressive behavior of fibre reinforced high-performance concrete subjected to elevated temperatures. *Cem. Concr. Res.* **2004**, *34*, 2215–2222. [[CrossRef](#)]
51. Chen, B.; Liu, J. Residual strength of hybrid-fibre-reinforced high-strength concrete after exposure to high temperatures. *Cem. Concr. Res.* **2004**, *34*, 1065–1069. [[CrossRef](#)]
52. Bezerra, C.S.; Maciel, P.S.; Corrêa, E.C.S.; Junior, P.R.R.S.; Aguilar, M.T.P.; Cetlin, P.R. Effect of high temperature on the mechanical properties of steel fibre-reinforced concrete. *Fibres* **2019**, *7*, 100. [[CrossRef](#)]
53. Chen, H.-G.; Liu, F.Y.; Sun, B.; Wang, M.; Cheng, P.-J. Impact of steel fibre dosage on mechanical properties of concrete under high temperature. *J. Chongqing Jiaotong Univ.* **2010**, *29*, 552–554.
54. Ismail, R.; Zakwan, F.A.A.; Petrus, C.; Marzuki, N.A.; Hashim, N.H.; Mustafa, M.F. Compressive behavior of steel fibre reinforced concrete after exposed to high temperatures. In *CIEC 2013*; Springer: Berlin/Heidelberg, Germany, 2014; pp. 731–740.
55. Colombo, M.; Di Prisco, M.; Felicetti, R. Mechanical properties of steel fibre reinforced concrete exposed at high temperatures. *Mater. Struct. Constr.* **2010**, *43*, 475–491. [[CrossRef](#)]

56. Li, L.; Zhang, R.; Jin, L.; Du, X.; Wu, J.; Duan, W. Experimental study on dynamic compressive behavior of steel fibre reinforced concrete at elevated temperatures. *Constr. Build. Mater.* **2019**, *210*, 673–684. [[CrossRef](#)]
57. Pliya, P.; Beaucour, A.L.; Noumowé, A. Contribution of cocktail of polypropylene and steel fibres in improving the behaviour of high strength concrete subjected to high temperature. *Constr. Build. Mater.* **2011**, *25*, 1926–1934. [[CrossRef](#)]
58. Choumanidis, D.; Badogiannis, E.; Nomikos, P.; Sofianos, A. The effect of different fibres on the flexural behaviour of concrete exposed to normal and elevated temperatures. *Constr. Build. Mater.* **2016**, *129*, 266–277. [[CrossRef](#)]
59. Jameran, A.; Ibrahim, I.S.; Yazan, S.H.S.; Rahim, S.N.A.A. Mechanical properties of steel-polypropylene fibre reinforced concrete under elevated temperature. *Procedia Eng.* **2015**, *125*, 818–824. [[CrossRef](#)]
60. Nielsen, C.V.; Biéanić, N. Residual fracture energy of high-performance and normal concrete subject to high temperatures. *Mater. Struct.* **2003**, *36*, 515–521. [[CrossRef](#)]
61. Menou, A.; Mounajed, G.; Boussa, H.; Pineaud, A.; Carre, H. Residual fracture energy of cement paste, mortar and concrete subject to high temperature. *Theor. Appl. Fract. Mech.* **2006**, *45*, 64–71. [[CrossRef](#)]
62. Lahoti, M.; Tan, K.H.; Yang, E.-H. A critical review of geopolymer properties for structural fire-resistance applications. *Constr. Build. Mater.* **2019**, *221*, 514–526. [[CrossRef](#)]
63. Amran, M.; Huang, S.-S.; Debbarma, S.; Rashid, R.S.M. Fire resistance of geopolymer concrete: A critical review. *Constr. Build. Mater.* **2022**, *324*, 126722. [[CrossRef](#)]
64. Ahmad, S.; Rasul, M.; Adekunle, S.K.; Al-Dulaijan, S.U.; Maslehuddin, M.; Ali, S.I. Mechanical properties of steel fibre-reinforced UHPC mixtures exposed to elevated temperature: Effects of exposure duration and fibre content. *Compos. Part B Eng.* **2019**, *168*, 291–301. [[CrossRef](#)]

Disclaimer/Publisher’s Note: The statements, opinions and data contained in all publications are solely those of the individual author(s) and contributor(s) and not of MDPI and/or the editor(s). MDPI and/or the editor(s) disclaim responsibility for any injury to people or property resulting from any ideas, methods, instructions or products referred to in the content.